Coherence, incoherence, and scaling along the *c* axis of $YBa_2Cu_3O_{6+x}$

C. C. Homes* and S. V. Dordevic
Department of Physics, Brookhaven National Laboratory, Upton, New York 11973, USA

D. A. Bonn, Ruixing Liang, and W. N. Hardy
Department of Physics and Astronomy, University of British Columbia, Vancouver, B.C., Canada V6T 2A6

T. Timusk
Department of Physics and Astronomy, McMaster University, Hamilton, Ontario, Canada L8S 4M1
(Received 17 December 2004; published 26 May 2005)

The optical properties of single crystals of $YBa_2Cu_3O_{6+x}$ have been examined along the *c* axis above and below the critical temperature (T_c) for a wide range of oxygen dopings. The temperature dependence of the optically determined value of the dc conductivity (σ_{dc}) in the normal state suggests a crossover from incoherent (hopping-type) transport at lower oxygen dopings ($x \lesssim 0.9$) to more coherent anisotropic three-dimensional behavior in the overdoped ($x \approx 0.99$) material at temperatures close to T_c. The assumption that superconductivity occurs along the *c* axis through the Josephson effect yields a scaling relation between the strength of the superconducting condensate ($\rho_{s,c}$, a measure of the number of superconducting carriers), the critical temperature, and the normal-state *c*-axis value for σ_{dc} just above T_c: $\rho_{s,c} \propto \sigma_{dc} T_c$. This scaling relation is observed along the *c* axis for all oxygen dopings, as well as several other cuprate materials. However, the Josephson coupling model does not *require* incoherent transport, so that the observed agreement with this model does not conflict with the normal-state results which point to coherent behavior at high oxygen dopings.

DOI: 10.1103/PhysRevB.71.184515 PACS number(s): 74.25.Gz, 74.72.Bk

I. INTRODUCTION

The cuprate-based high-temperature superconductors all share the common feature that the superconductivity is thought to originate within the highly conducting copper-oxygen planes. The conductivity perpendicular to the planes along the *c* axis is much poorer and is in fact activated in many cuprates; the resulting transport is due to hopping along this direction and the large anisotropy in the resistivity results in the two-dimensional (2D) nature of these systems.[1] The importance of the 2D character of these materials as a necessary prerequisite for superconductivity has been discussed,[2] and it has recently been suggested that upon entering the superconducting state a dimensional crossover from two to three dimensions occurs.[3,4] Transport measurements on a number of cuprate systems suggest that such a dimensional crossover may occur in the normal state in response to carrier doping in the copper-oxygen planes.[5–10] A convenient system to examine is $YBa_2Cu_3O_{6+x}$ (YBCO), where the oxygen doping determines not only the in-plane carrier concentration, but also the nature of the *c*-axis transport. This material is one of the most thoroughly studied, and there have been numerous reports of the response of the physical properties to changes in oxygen doping, including transport[5,11] and optical techniques,[12–19] to name a few.

In YBCO oxygen dopings below the optimal value ($x = 0.95$) for the critical temperature T_c, the dc resistivity along the *c* axis is $\rho_c \propto T^{\alpha}$, where $\alpha \lesssim -1$, indicative of activated behavior. In these underdoped materials, the anisotropy between the *a-b* planes and the *c* axis, as gauged by the resistivity, is quite large: $\rho_c/\rho_a \gtrsim 65$ at room temperature, and increases rapidly with decreasing temperature to $\rho_c/\rho_a \geqslant 3000$ ($x \lesssim 0.70$) just above T_c.[11] For these reasons, transport along the *c* axis in the normal state in the underdoped materials is governed by hopping and is considered to be incoherent; below T_c superconductivity normal to the planes is thought to involve Josephson coupling.[20–22] However, as the material becomes nearly stoichiometric, or "overdoped" ($x \approx 0.99$), the *c*-axis properties change dramatically. Unlike in the underdoped systems, the resistivity rises linearly with *T*, although with a large, temperature-independent component. Furthermore, $\rho_c/\rho_a \lesssim 30$ at room temperature, and is nearly temperature independent in the normal state,[11] characteristic of an anisotropic three-dimensional (3D) metal. This behavior is even more pronounced in the Ca-doped material.[23] In addition, the anisotropic resistivity of the double-chain material $YBa_2Cu_4O_8$ also suggests an incoherent-to-coherent crossover in the out-of-plane behavior.[8] This suggests that transport along the *c* axis of YBCO is becoming more coherent at high oxygen dopings, and that a crossover from 2D to 3D behavior may occur; this could have important consequences for the nature of the superconductivity.

In this work we examine the optical properties along the *c* axis of $YBa_2Cu_3O_{6+x}$ for a wide range of oxygen dopings in the normal and superconducting states. The normal-state transport suggests that a dimensional crossover may occur in the overdoped YBCO samples. The strength of the condensate along the *c* axis is consistent with the Josephson coupling between the planes. However, because the Josephson effect may be observed for both coherent and incoherent transport along the *c* axis (tunnel and nontunnel junctions), the condensate does not necessarily favor incoherent transport in the overdoped material, where the normal-state properties suggest the system tends toward coherent behavior.

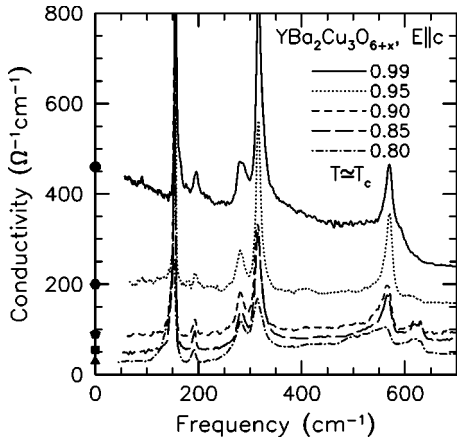

FIG. 1. The real part of the optical conductivity for light polarized along the c axis of $YBa_2Cu_3O_{6+x}$ at $T \gtrsim T_c$ for a variety of oxygen dopings. The extrapolated values of the dc conductivity $\sigma_{dc}=\sigma_1(\omega \to 0)$ are shown as symbols. The most heavily doped regime ($x=0.99$) is representative of a weakly metallic system and the conductivity displays a Drude-like frequency dependence. The lowest oxygen concentration shown here ($x=0.80$) is in the pseudogap regime, with an activated frequency response.

II. EXPERIMENT

Large, twinned single crystals of YBCO were grown by a flux method in yttria-stabilized zirconia crucibles[24] and subsequently reannealed to a variety of oxygen contents from $x=0.50 \to 0.99$. The T_cs are sharply defined and vary over a large range, from a low of $T_c=53$ K in the most underdoped material ($x=0.50$) to a maximum of $T_c=93.2$ K in the optimally doped material ($x=0.95$). In the most overdoped sample ($x \gtrsim 0.99$), T_c is suppressed somewhat to $T_c \approx 90$ K. The reflectance polarized along the c axis was measured over a wide frequency range and at a variety of temperatures using an overfilling technique.[25] The real part of the optical conductivity $\sigma_1(\omega)$ was determined from a Kramers-Kronig analysis of the reflectance.

III. RESULTS AND DISCUSSION

A. Normal state

The optical properties along the c axis have been thoroughly investigated by us and others,[12–14,16–19] and will be discussed only briefly. The optical conductivity of YBCO is shown along the c axis in Fig. 1 for $T \gtrsim T_c$ at a variety of oxygen dopings. In the overdoped regime the conductivity has a metallic temperature and frequency dependence. However, with decreasing doping a pseudogap develops, and a nonmetallic activated response is observed. A convenient connection between the optical properties and transport is that $\sigma_{dc} \equiv \sigma_1(\omega \to 0)$ as indicated in the plot and listed in Table I (for $T \gtrsim T_c$). The extrapolated values for the resistivity ρ_{dc} along the c axis are shown in Fig. 2 for a variety of oxygen dopings at room temperature and $T \gtrsim T_c$. At room temperature the resistivity increases exponentially with decreasing doping, $\rho_c \propto \rho_0 e^{-ax}$, throughout the entire doping range. At low temperature the resistivity is observed to increase with decreasing temperature for $x \lesssim 0.85$, in agreement with the activated response observed in transport; once again the resistivity varies exponentially with doping. However, for $x \gtrsim 0.9$ the resistivity decreases dramatically with increased doping and no longer follows the simple exponential relation. In addition, the temperature response of the resistivity is now "metallic," particularly so for the overdoped sample.[5] This change in behavior also occurs close to the Mott maximum value for metallic behavior (ML), estimated to be $\rho_c \approx 10$ mΩ cm in these materials.[26] The overdoped material is clearly the most metallic, and displays a Drude-like conductivity, an important result that was noted in earlier studies.[17] The Drude model for the dielectric function describes the properties of a simple metal quite well, $\tilde{\epsilon}(\omega) = \epsilon_\infty - \omega_p^2/[\omega(\omega + i\Gamma)]$, where ω_p is the classical plasma fre-

TABLE I. The doping-dependent values in $YBa_2Cu_3O_{6+x}$ for the critical temperature (T_c), and c axis far-infrared conductivity (σ_{dc}) measured just above T_c, the strength of the condensate, expressed as a plasma frequency ($\omega_{ps,c}$), and the penetration depth [$\lambda_c = 1/(2\pi\omega_{ps,c})$].

x	T_c (K)	σ_{dc} (Ω^{-1} cm^{-1})[a]	$\omega_{ps,c}$ (cm^{-1})	λ_c (μm)
0.50	53	9±2	204±20	7.80
0.60	58	12±2	244±20	6.52
0.70	63	14±2	315±30	5.05
0.80	78	27±4	465±35	3.42
0.85	89	47±7	790±50	2.01
0.90	91.5	88±10	1003±60	1.59
0.95	93.2	220±20	1580±70	1.01
0.99	90	450±30	2070±90	0.77

[a]Taken at $\omega \to 0$ limit for $T \gtrsim T_c$.

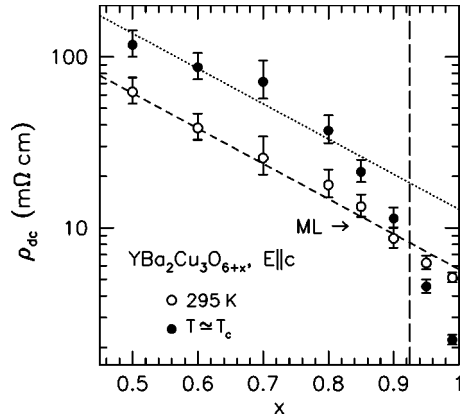

FIG. 2. Resistivity $\rho_{dc}=1/\sigma_1(\omega \to 0)$ for $YBa_2Cu_3O_{6+x}$ along the c axis at 295 K and $T \gtrsim T_c$ as a function of oxygen doping. At room temperature, ρ_{dc} increases exponentially with decreasing oxygen doping, as indicated by the dashed line. However, for $T \gtrsim T_c$, a linear fit applies only to the dopings between $0.50 \leqslant x \leqslant 0.85$, or the underdoped region (dotted line); values for $x > 0.9$ fall below this line. This indicates that in the underdoped region resistivity increases with decreasing temperature, while in the overdoped region, precisely the opposite behavior is observed at roughly the Mott minimum limit for metallic conductivity (ML).

quency, $\Gamma = 1/\tau$ is the scattering rate, and ϵ_∞ is a high-frequency contribution. The Drude conductivity is $\sigma_1(\omega) = \sigma_{dc}/(1+\omega^2\tau^2)$, which has the form of a Lorentzian centered at zero frequency with a width at half maximum of $1/\tau$. For $T \gtrsim T_c$, the optical conductivity of the overdoped system shown in Fig. 1 does have a Drude-like frequency response, $\sigma_1(\omega) \propto 1/\omega^2$. In addition $\sigma_{dc} \equiv \sigma_1(\omega \rightarrow 0) \approx 450\ \Omega^{-1}\,\mathrm{cm}^{-1}$ for $T \gtrsim T_c$ is well above the Mott minimum value for metallic conductivity of $\approx 100\ \Omega^{-1}\,\mathrm{cm}^{-1}$ in these materials.

Previous investigations of overdoped systems resulted in large values for both the plasma frequency $\omega_{p,c}$ ($\gtrsim 4000\ \mathrm{cm}^{-1}$) and the scattering rate $1/\tau_c$ ($\gtrsim 1000\ \mathrm{cm}^{-1}$).[12,17] A principal objection to coherent transport along the *c* axis has been the large values for $1/\tau_c$ which lead to mean free paths that are substantially less than a lattice spacing.[1] If the *c*-axis conductivity is modeled using a two-component approach (Drude component to model free carriers, plus Lorentzian oscillators to represent bound excitations), then it is possible to estimate the *c*-axis plasma frequency and scattering rate. This approach yields values of $\omega_{p,c} \simeq 3200\ \mathrm{cm}^{-1}$ and $1/\tau_c \simeq 380\ \mathrm{cm}^{-1}$ at 100 K, smaller than previously observed values.[27] These results may be compared to the values in the copper-oxygen planes along the *a* axis for the overdoped material[28] of $\omega_{p,a} \simeq 10\,000\ \mathrm{cm}^{-1}$ and $1/\tau_a \simeq 120\ \mathrm{cm}^{-1}$. The resistivity anisotropy is then expected to be $\rho_c/\rho_a = (\omega_{p,a}^2\tau_a)/(\omega_{p,c}^2\tau_c) \gtrsim 30$, where $\omega_{p,a}^2/\omega_{p,c}^2 \simeq 10$, which is in good agreement with band-structure estimates.[29] Furthermore, taking $v_F = 7\times 10^6$ cm/s gives a mean free path along the *c* axis ($l_c = v_F\tau_c$) of $l_c \simeq 60$ Å, which is more than five times the size of the unit cell, suggesting the possibility of coherent (Bloch-Boltzmann) transport in the overdoped material for $T \gtrsim T_c$.[17] The increasingly coherent transport along the *c* axis has also been discussed in relation to the strength of the inelastic scattering in the copper-oxygen planes.[30]

B. Superconducting state

In YBCO the onset of superconductivity is accompanied by the dramatic formation of a plasma edge in the reflectance along the *c* axis for all the oxygen dopings studied.[13,14] In the copper-oxide superconductors, the order parameter is thought to originate within the planes, with bulk superconductivity achieved through coherent pair tunneling between the planes occurring from the Josephson effect.[31] In such a case the *c*-axis penetration depth λ_c is determined by the Josephson current density J_c and is $\lambda_c^2 = \hbar c^2/8\pi^2 deJ_c \propto 1/dJ_c$, where *d* is the separation between the planes.[32,33] In the BCS theory, J_c is related to the energy gap $\Delta(T)$ and the tunneling resistance per unit area in the normal state R_n by[34]

$$J_c = \frac{\pi\Delta(T)}{2eR_n}\tanh\left[\frac{\Delta(T)}{2k_BT}\right]. \tag{1}$$

Adopting the BCS isotropic *s*-wave gap weak-coupling value of $\Delta(T \ll T_c) \simeq 1.76 k_B T_c$ and assuming that $R_n = \rho_{dc} d$, then $J_c \propto T_c/R_n$ at low temperature, and $1/\lambda_c^2 \propto \sigma_{dc} T_c$, where σ_{dc} is the extrapolated dc conductivity along the *c* axis in the normal state ($T \gtrsim T_c$).[20,21] From $1/\lambda = 2\pi\omega_{ps}$, the strength of the condensate is $\rho_s \equiv \omega_{ps}^2$, yielding

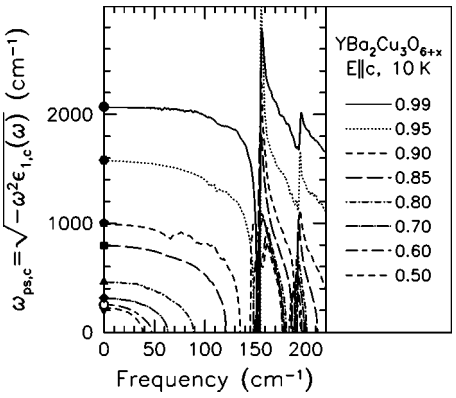

FIG. 3. The doping-dependent behavior of $\sqrt{-\omega^2\epsilon_{1,c}(\omega)}$ for $T \ll T_c$. In the $\omega \rightarrow 0$ limit this quantity is the plasma frequency of the condensate along the *c* axis, $\omega_{ps,c}$. The low-frequency extrapolation employed in the Kramers-Kronig analysis below $\simeq 40\ \mathrm{cm}^{-1}$ is included as a guide to the eye. The strength of the plasma frequency is decreasing dramatically with decreasing oxygen doping (Table I).

$$\rho_{s,c} \simeq 65\sigma_{dc}T_c, \tag{2}$$

where the right and left hand side of the expression have units of cm^{-2}. We note that several other workers have arrived at a similar relationship based on different assumptions.[35,36] If the clean limit is assumed (all the normal-state carriers collapse into the condensate), then for $T \ll T_c$ the response of the dielectric function is purely real, $\tilde{\epsilon}(\omega) \equiv \epsilon_1(\omega) = \epsilon_\infty - \omega_{ps}^2/\omega^2$, so that the plasma frequency of the condensate is $\omega_{ps,c}^2 = -\omega^2\epsilon_{1,c}(\omega)$ in the limit of $\omega \rightarrow 0$. The frequency dependence of $\sqrt{-\omega^2\epsilon_{1,c}(\omega)}$ is shown in Fig. 3 for a variety of oxygen dopings for $T \ll T_c$. The low-frequency extrapolations employed in the Kramers-Kronig analysis of the reflectance (typically below 40 cm^{-1}) are included to allow the $\omega \rightarrow 0$ values to be determined more easily. The estimate of $\omega_{ps,c}$ assumes that the response of $\epsilon_{1,c}(\omega)$ at low frequency is dominated by the superconducting condensate. The overdoped material is known to have a large amount of low-frequency residual conductivity for $T \ll T_c$, which may lead to an overestimate of $\omega_{ps,c}$. However, one of us (S.V.D.) has developed a self-consistent technique[30] whereby $\epsilon_{2,c}(\omega)$ may be used to calculate corrections to $\epsilon_{1,c}(\omega)$ and subsequently allow an accurate determination of the value of $\omega_{ps,c}$. The corrections are typically small (less than a few %); the values for $\omega_{ps,c}$ are listed in Table I, and are in good agreement with values recently obtained from zero-field electron spin resonance (ESR) studies.[37]

The optically determined values for the superfluid density $\rho_{s,c}$ versus $\sigma_{dc}T_c$ for YBCO are shown in the log-log plot in Fig. 4. In addition, the *c*-axis results for $YBa_2Cu_4O_8$,[21] $Tl_2Ba_2CuO_{6+\delta}$,[38] $HgBa_2CuO_{4+\delta}$,[39] and $La_{2-x}Sr_xCuO_4$ (Ref. 39) are also shown. All the points fall on a line approximated by the scaling relation $\rho_{s,c} \simeq 35\sigma_{dc}T_c$, which is close to the result from Josephson coupling.[39] In the log-log representation of Fig. 4, the numerical constant in the scaling relation is the offset of the line. The line may be shifted by assuming different ratios between 2Δ and k_BT_c; the initial value of $\simeq 65$ was based on the weak-coupling value of $2\Delta/k_BT_c$

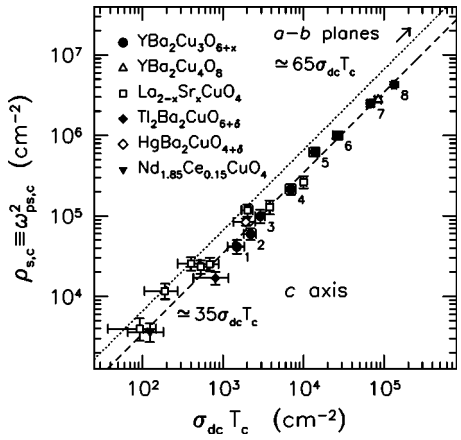

FIG. 4. The optically determined strength of the condensate $\rho_{s,c}$ vs $\sigma_{dc}T_c$ along the *c* axis in $YBa_2Cu_3O_{6+x}$ for various oxygen dopings (labeled from the lowest to the highest oxygen doping in ascending order), as well as results for other single and double-layer copper-oxide superconductors. The data are described reasonably well by the dashed line, $\rho_{s,c} \simeq 35\sigma_{dc}T_c$. The dotted line is the result of Josephson coupling assuming a BCS isotropic gap in the weak-coupling limit, $\rho_{s,c} \simeq 65\sigma_{dc}T_c$. The arrow indicates that the *a-b* plane data may also be scaled on the same dashed line as the *c* axis data (see Ref. 39).

$\simeq 3.5$, while the observed value of $\simeq 35$ implies a smaller ratio $2\Delta/k_BT_c \simeq 2$. Previous studies along the *c* axis of the cuprate materials considered the dependence of $\rho_{s,c}$ with σ_{dc};[30] underdoped materials followed this scaling behavior reasonably well, but deviations were observed for optimal and overdoped materials. It is surprising that the Josephson coupling result describes the scaling behavior along the *c* axis as well as it does given the assumption of a BCS *s*-wave isotropic energy gap, when there is strong evidence to suggest that the energy gap in copper-oxygen planes of YBCO is *d* wave in nature and contains nodes.[40,41] A possible explanation may be that the *c*-axis properties are particularly sensitive to the zone boundary $(\pi,0)$, $(0,\pi)$ part of the Fermi surface where the superconducting gap is observed to open at T_c in optimally doped materials.[23,42–46] In this case the *d*-wave nature of the superconducting gap is not probed and the assumption of an isotropic gap is qualitatively correct, yielding a reasonable agreement between theory and experiment. The Josephson result might have been expected for the underdoped materials where the transport along the *c* axis was activated and considered incoherent. However, it is less obvious for the optimally and overdoped systems; the overdoped material in particular gave indications of anisotropic 3D normal-state transport, and as such some deviation from this behavior might have been expected. Thus, it would be tempting to assume that the observed scaling $\rho_{s,c} \propto \sigma_{dc}T_c$ along the *c* axis justifies the view that the coupling between the planes is always incoherent. However, it is important to note that both tunnel junctions [superconductor-insulator-superconductor (SIS)] in the case considered here, as well as nontunnel junctions [superconductor-normal-superconductor (SNS)] can show the Josephson effect with a nearly identical Josephson current.[47–49] As a result, the qualitative agreement with the Josephson coupling model does not conflict with the normal-state results, which indicate that the transport is becoming more coherent at high oxygen dopings.

IV. CONCLUSIONS

The optical and transport properties in the normal state of YBCO suggest that the material shows signs of anisotropic 3D metallic transport at high oxygen dopings for $T \simeq T_c$. A scaling relation $\rho_{s,c} \simeq 35\sigma_{dc}T_c$ is observed along the *c* axis, in agreement with the result expected from Josephson coupling in the BCS weak limit case. We note that the Josephson coupling model does not require incoherent transport, suggesting that the transport may indeed tend towards more coherent behavior in YBCO at higher oxygen dopings.

ACKNOWLEDGMENTS

We would like to thank D. N. Basov, S. L. Cooper, V. J. Emery, J. C. Irwin, M. V. Klein, T. Rõõm, M. Strongin, and J. J. Tu for helpful discussions. This work was supported by the Natural Sciences and Engineering Research Council of Canada, the Canadian Institute for Advanced Research, and the Department of Energy under Contract No. DE-AC02-98CH10886.

*Electronic address: homes@bnl.gov

[1] S. L. Cooper and K. E. Gray, in *Physical Properties of High-Temperature Superconductors IV*, edited by D. M. Ginsberg (World Scientific, Singapore, 1994), pp. 61–188.
[2] P. W. Anderson, Science **279**, 1196 (1998).
[3] T. Valla, P. D. Johnson, Z. Yusof, B. Wells, Q. Li, S. M. Loureiro, R. J. Cava, M. Mikami, Y. Mori, M. Yoshimura, and T. Sasaki, Nature (London) **417**, 627 (2002).
[4] A. Menzel, R. Beer, and E. Bertel, Phys. Rev. Lett. **89**, 076803 (2002).
[5] T. Ito, H. Takagi, S. Ishibashi, T. Ido, and S. Uchida, Nature (London) **350**, 596 (1991).
[6] Y. Nakamura and S. Uchida, Phys. Rev. B **47**, R8369 (1993).
[7] H. L. Kao, J. Kwo, H. Takagi, and B. Batlogg, Phys. Rev. B **48**, R9925 (1993).
[8] N. E. Hussey, K. Nozawa, H. Takagi, S. Adachi, and K. Tanabe, Phys. Rev. B **56**, R11423 (1997).
[9] T. Schneider, cond-mat/0205304 (unpublished).
[10] T. Schneider and H. Keller, New J. Phys. **6**, 144 (2004).
[11] K. Takenaka, K. Mizuhashi, H. Takagi, and S. Uchida, Phys. Rev. B **50**, R6534 (1994).
[12] S. L. Cooper, P. Nyhus, D. Reznik, M. V. Klein, W. C. Lee, D. M. Ginsberg, B. W. Veal, A. P. Paulikas, and B. Dabrowski, Phys. Rev. Lett. **70**, 1533 (1993).
[13] C. C. Homes, T. Timusk, R. Liang, D. A. Bonn, and W. N. Hardy, Phys. Rev. Lett. **71**, 1645 (1993).

[14] C. C. Homes, T. Timusk, D. A. Bonn, R. Liang, and W. N. Hardy, Physica C **254**, 265 (1995).
[15] C. C. Homes, T. Timusk, D. A. Bonn, R. Liang, and W. N. Hardy, Can. J. Phys. **73**, 663 (1995).
[16] C. C. Homes, S. Kamal, D. A. Bonn, R. Liang, W. N. Hardy, and B. P. Clayman, Physica C **296**, 230 (1998).
[17] J. Schützmann, S. Tajima, S. Miyamoto, and S. Tanaka, Phys. Rev. Lett. **73**, 174 (1994).
[18] J. Schützmann, S. Tajima, S. Miyamoto, Y. Sato, and R. Hauff, Phys. Rev. B **52**, 13665 (1995).
[19] S. Tajima, J. Schützmann, S. Miyamoto, I. Terasaki, Y. Sato, and R. Hauff, Phys. Rev. B **55**, 6051 (1997).
[20] T. Shibauchi, H. Kitano, K. Uchinokura, A. Maeda, T. Kimura, and K. Kishio, Phys. Rev. Lett. **72**, 2263 (1994).
[21] D. N. Basov, T. Timusk, B. Dabrowski, and J. D. Jorgensen, Phys. Rev. B **50**, R3511 (1994).
[22] R. J. Radtke and K. Levin, Physica C **250**, 282 (1995).
[23] C. Bernhard, D. Munzar, A. Wittlin, W. König, A. Golnik, C. T. Lin, M. Kläser, T. Wolf, G. Müller-Vogt, and M. Cardona, Phys. Rev. B **59**, R6631 (1999).
[24] R. Liang, P. Dosanjh, D. A. Bonn, D. J. Barr, J. F. Carolan, and W. N. Hardy, Physica C **195**, 51 (1992).
[25] C. C. Homes, M. Reedyk, D. Crandles, and T. Timusk, Appl. Opt. **32**, 2972 (1993).
[26] N. F. Mott and E. A. Davis, *Electronic Processes in Non-Crystalline Materials* (Clarendon, Oxford, 1971).
[27] In the Drude-Lorentz or two-component fit, in addition to the Drude term, Lorentzian oscillators with frequency, width, and effective plasma frequency ω_i, γ_i, and $\omega_{p,i}$ have also been used to fit the B_{1u} infrared active lattice modes (Ref. 14) as well as a number of other oscillators in the mid and near infrared: $\omega_1 = 800$, $\gamma_1 = 2580$, $\omega_{p1} = 5422$; $\omega_2 = 2400$, $\gamma_2 = 1540$, $\omega_{p2} = 1840$; $\omega_3 = 1.2 \times 10^4$, $\gamma_3 = 1.4 \times 10^4$, $\omega_{p3} = 1.9 \times 10^4$. All units are in cm^{-1}.
[28] T. Rõõm (private communication).
[29] P. B. Allen, W. E. Pickett, and H. Krakauer, Phys. Rev. B **37**, 7482 (1988).
[30] S. V. Dordevic, E. J. Singley, D. N. Basov, S. Komiya, Y. Ando, E. Bucher, C. C. Homes, and M. Strongin, Phys. Rev. B **65**, 134511 (2002).
[31] A. A. Abrikosov, Phys. Rev. B **57**, 7488 (1998).
[32] L. N. Bulaevskii, Sov. Phys. JETP **37**, 598 (1973).
[33] W. E. Lawrence and S. Doniach, in *Proceedings of the 12th International Conference on Low Temperature Physics, Kyoto, 1970*, edited by E. Kando (Academic, Tokyo, 1971), pp. 361–362.
[34] V. Ambegaokar and A. Baratoff, Phys. Rev. Lett. **10**, 486 (1963).
[35] R. A. Smith and V. Ambegaokar, Phys. Rev. B **45**, 2463 (1992).
[36] S. Chakravarty, H.-Y. Kee, and E. Abrahams, Phys. Rev. Lett. **82**, 2366 (1993). The superfluid density was calculated to be $\rho_{s,c} = 4\pi\sigma_c(T^*)T^*\{b_2(p+1)[u_s - u_n]/p\}$. The expression in the curly brackets, described in detail in the reference, is assumed to be a universal constant. For $T^* \simeq T_c$, then $\rho_{s,c} \propto \sigma_{dc}T_c$, which is similar to the Josephson result.
[37] T. Pereg-Barnea, P. J. Turner, R. Harris, G. K. Mullins, J. S. Bobowski, M. Raudsepp, R. Liang, D. A. Bonn, and W. N. Hardy, Phys. Rev. B **69**, 184513 (2004).
[38] D. N. Basov, S. I. Woods, A. S. Katz, E. J. Singley, R. C. Dynes, M. Xu, D. G. Hinks, C. C. Homes, and M. Strongin, Science **283**, 49 (1999).
[39] C. C. Homes, S. V. Dordevic, M. Strongin, D. A. Bonn, R. Liang, W. N. Hardy, S. Komlya, Y. Ando, G. Yu, N. Kaneko, X. Zhao, M. Greven, D. N. Basov, and T. Timusk, Nature (London) **430**, 539 (2004).
[40] W. N. Hardy, D. A. Bonn, D. C. Morgan, R. Liang, and K. Zhang, Phys. Rev. Lett. **70**, 3999 (1993).
[41] H. Ding, M. R. Norman, J. C. Campuzano, M. Randeria, A. F. Bellman, T. Yokoya, T. Takahashi, T. Mochiku, and K. Kadowaki, Phys. Rev. B **54**, R9678 (1996).
[42] S. Chakravarty, A. Sudbo, P. W. Anderson, and S. Strong, Science **261**, 337 (1993).
[43] T. Xiang and J. M. Wheatley, Phys. Rev. Lett. **77**, 4632 (1996).
[44] D. van der Marel, Phys. Rev. B **60**, R765 (1999).
[45] L. B. Ioffe and A. J. Millis, Science **285**, 1241 (1999).
[46] D. N. Basov, C. C. Homes, E. J. Singley, M. Strongin, T. Timusk, G. Blumberg, and D. van der Marel, Phys. Rev. B **63**, 134514 (2001).
[47] I. O. Kulik and A. N. Omel'yanchuk, JETP Lett. **21**, 96 (1975).
[48] K. K. Likharev, Rev. Mod. Phys. **51**, 101 (1979).
[49] A. A. Golubov, M. Y. Kupriyanov, and E. Il'ichev, Rev. Mod. Phys. **76**, 411 (2004).